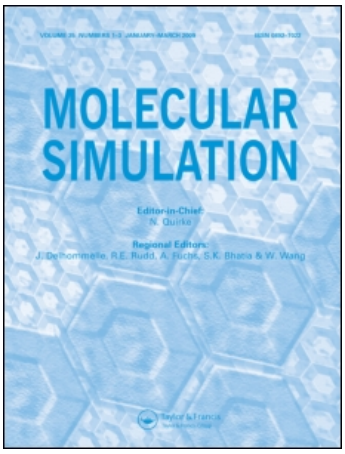

Molecular Simulation
Publication details, including instructions for authors and subscription information:
http://www.informaworld.com/smpp/title~content=t713644482

A Duhamel approach for the Langevin equations with holonomic constraints

B. Kallemov [a]; G. H. Miller [ab]; D. Trebotich [bc]
[a] Department of Applied Science, University of California, Davis, CA, USA [b] Applied Numerical Algorithms Group, Lawrence Berkeley National Laboratory, Berkeley, CA, USA [c] Center for Applied Scientific Computing, Lawrence Livermore National Laboratory, Livermore, CA, USA

First Published:May2009

To cite this Article Kallemov, B., Miller, G. H. and Trebotich, D.(2009)'A Duhamel approach for the Langevin equations with holonomic constraints',Molecular Simulation,35:6,440 — 447
To link to this Article: DOI: 10.1080/08927020802541327
URL: http://dx.doi.org/10.1080/08927020802541327

Molecular Simulation
Vol. 35, No. 6, May 2009, 440–447

Taylor & Francis
Taylor & Francis Group

A Duhamel approach for the Langevin equations with holonomic constraints

B. Kallemov[a1], G.H. Miller[ab]* and D. Trebotich[bc2]

[a]*Department of Applied Science, University of California, Davis, CA, USA;* [b]*Applied Numerical Algorithms Group, Lawrence Berkeley National Laboratory, Berkeley, CA, USA;* [c]*Center for Applied Scientific Computing, Lawrence Livermore National Laboratory, Livermore, CA, USA*

(*Received 4 September 2008; final version received 8 October 2008*)

To simulate polymer flows in microscale environments we have developed a numerical method that couples stochastic particle dynamics with an efficient incompressible Navier–Stokes solver. Here, we examine properties of the particle solver alone. We derive a Duhamel-form stochastic particle method for freely jointed polymers and demonstrate that it achieves 2-order weak convergence and 3/2-order strong convergence with holonomic constraints. For time steps approaching the $1/\gamma$ relaxation time, our method displays greatly enhanced stability relative to comparable solvers based on linearised dynamics. Under these same conditions, our method has solution errors that are approximately six orders of magnitude smaller than that for the linearised algorithm.

Keywords: stochastic particle dynamics; RATTLE; particle-fluid coupling

1. Introduction

The dynamics of a continuum fluid with discrete embedded polymers is important for certain microfluidic applications (e.g. so-called lab-on-a-chip devices used for biochemical analysis and detection) and for modelling viscoelastic phenomena in the dilute limit. Towards this end, we proposed a fluid–particle coupling strategy [12] that uses Brownian dynamics to approximate molecular-level fluid–polymer interactions. In subsequent work (e.g. [7]) the time stability of the scheme was improved, and constraints such as the non-crossing constraint for polymer–polymer interaction were considered. In this short paper, we address the accuracy of our scheme. We work here in the framework of a freely-jointed chain (no polymer–polymer interactions), we consider the fluid velocity field to be prescribed, and we do not consider any rigid domain boundaries. In the context of rigid constraint dynamics (vs. soft penalty method constraints), these omitted interactions will diminish the order of the local discretisation error.

Recently, [13] proposed a weak second-order stochastic particle dynamics approach that is broadly similar to ours as described in [7,12]. Our approach differs from theirs in our handling of the fluid–particle coupling, and our use of a Duhamel type discretisation that recovers certain limiting behaviour exactly.

The main points of this paper are two. First, the methods of stochastic ODE analysis commonly used for these problems employ a linearisation of the ODEs. We derive here an alternative formulation of such methods, which does not rely on linearisation. We demonstrate the advantages of this new approach for stability and accuracy in the large time-step limit. Second, we go beyond the usual weak analysis to show the strong rate of convergence. Accuracy in the weak sense relies on a large ensemble of stochastic paths – akin to the reliance on the ergotic hypothesis by molecular dynamics (MD) theory. Our motivating application is a multiscale simulation that combines polymer dynamics with fluid dynamics. Owing to the large computational expense of the fluid solvers, it is impractical to simulate a large enough ensemble of states for the weak measure of error to apply. By contrast, the strong sense of error applies to the given paths, i.e. for any operational definition of the underlying stochastic processes; a second-order strong method is reasonably expected to attain second-order accuracy. We show that our approach is weak 2-order accurate and order 3/2 strong with holonomic constraints.

We model a polymer as a collection of coupled point masses, each subject to the Langevin equation of motion

$$\ddot{\mathbf{x}}_\alpha = \gamma(\mathbf{u} - \dot{\mathbf{x}}_\alpha) + \frac{1}{m_\alpha}\mathbf{F}(\mathbf{x}_\alpha) + \sigma\boldsymbol{\xi}_\alpha(t). \tag{1}$$

Here, $\mathbf{x} = \mathbf{x}(t)$ is the position of the αth particle with mass m_α; $\mathbf{u}$ is fluid velocity; $\mathbf{F}(x)$ is the interparticle force; $\gamma > 0$ is the friction coefficient; and $\boldsymbol{\xi}(t)$ is a white noise representing stochastic thermal bombardment by the solvent. The constant σ is given by $\sqrt{2\gamma k_B T/m_\alpha}$ with k_B being Boltzmann's constant and T the temperature.

In this work, we will use Kramers' polymer model, which represents a polymer as points governed by (1) with the interparticle force $\mathbf{F}$ chosen to enforce the constraint

*Corresponding author. Email: grgmiller@ucdavis.edu

ISSN 0892-7022 print/ISSN 1029-0435 online

DOI: 10.1080/08927020802541327
http://www.informaworld.com

of fixed interparticle spacing. The general idea is to add into equations of motion constraint forces that can be expressed as:

$$\mathbf{G}_\alpha = -\sum_\beta \lambda_{\alpha\beta}(t)\nabla_\alpha \theta_{\alpha\beta}, \tag{2}$$

$$\theta_{\alpha\beta} = \frac{1}{2}\left(\|\mathbf{x}_\alpha - \mathbf{x}_\beta\|^2 - a^2\right) = 0, \tag{3}$$

where particles of index β are neighbours of particle α; $\lambda_{\alpha\beta}$ are Lagrange multipliers chosen to satisfy the constraints; and a = const. is the spacing between adjacent particles.

2. Numerical method

A numerical method for the integration of (1) was given without proof in [12]. Here, a derivation of those equations is given. We begin by expressing the second-order SDE as a system of first-order equations in the Duhamel form:

$$\begin{aligned} \mathrm{d}\mathbf{x}(t) &= \mathrm{e}^{-\gamma t}\mathbf{z}(t)\mathrm{d}t, \\ \mathrm{d}\mathbf{z}(t) &= \gamma \mathrm{e}^{\gamma t}\mathbf{u}(t,\mathbf{x}(t))\mathrm{d}t + \sigma \mathrm{e}^{\gamma t}\mathrm{d}\mathbf{W}, \end{aligned} \tag{4}$$

and

$$\begin{aligned} \mathbf{x}(t) &= \mathbf{x}(0) + \int_0^t \mathrm{e}^{-\gamma s}\mathbf{z}(s)\mathrm{d}s, \\ \mathbf{z}(t) &= \mathbf{z}(0) + \int_0^t \gamma \mathrm{e}^{\gamma s}\mathbf{u}(s,\mathbf{x}(s))\mathrm{d}s + \int_0^t \sigma \mathrm{e}^{\gamma s}\mathrm{d}\mathbf{W}_s, \end{aligned} \tag{5}$$

where $\mathbf{z} = \mathbf{v}\mathrm{e}^{\gamma t}$; $\mathbf{W}(t)$ is a standard Weiner process; and $\mathrm{d}\mathbf{W} = \boldsymbol{\xi}\mathrm{d}t$.

We then expand our equations of motion in an Itô–Taylor series, using the Itô calculus for stochastic ODEs [4]:

$$\begin{aligned} Y &= U(t, X(t)), \\ \mathrm{d}X(t) &= f(t)\mathrm{d}t + g(t)\mathrm{d}W, \\ \mathrm{d}Y(t) &= \left[\frac{\partial U}{\partial t} + \frac{\partial U}{\partial X}f(t) + \frac{1}{2}\frac{\partial^2 U}{\partial X^2}g^2(t)\right]\mathrm{d}t + \frac{\partial U}{\partial X}g\mathrm{d}W. \end{aligned} \tag{6}$$

Application of this stochastic chain rule requires care to account for all dependence on stochastic variables. In real systems, the fluid $\mathbf{u}$ is driven by a nonlinear stochastic coupling. Additionally, every fluid element undergoes thermal fluctuation, whether expressed explicitly as a Brownian force or not. However, the average magnitude of such fluctuations in a given volume scales as the inverse of the number of atoms in that volume. At the scales of length with which we are concerned, the continuum fluid motion $\mathbf{u}$ is smooth. Thus, in our analysis, the stochastic dependence of $\mathbf{u}$ is through the particle position $\mathbf{x}$ only: $\mathbf{u} = \mathbf{u}(t, \mathbf{x}(t))$.

With this assumption, application of the Itô formula to the $\mathbf{W}$-dependent integrands of (5) gives:

$$\begin{aligned} \mathrm{e}^{-\gamma s}\mathbf{z}(s) = \mathbf{z}(0) &+ \int_0^s \left[-\gamma \mathrm{e}^{-\gamma s_1}\mathbf{z}(s_1) + \gamma \mathbf{u}(s_1, \mathbf{x}(s_1))\right]\mathrm{d}s_1 \\ &+ \sigma \int_0^s \mathrm{d}\mathbf{W}_{s_1}, \end{aligned} \tag{7}$$

$$\begin{aligned} \gamma \mathrm{e}^{\gamma s}\mathbf{u}(s,\mathbf{x}(s)) = \gamma \mathbf{u}(0,\mathbf{x}(0)) &+ \int_0^s \left[\gamma^2 \mathrm{e}^{\gamma s_1}\mathbf{u}(s_1,\mathbf{x}(s_1))\right. \\ &\left. + \gamma \mathrm{e}^{\gamma s_1}\frac{D\mathbf{u}(s_1,\mathbf{x}(s_1))}{Ds_1}\right]\mathrm{d}s_1. \end{aligned}$$

Substituting expansions (7) into (5) gives:

$$\begin{aligned} \mathbf{x}(t) = \mathbf{x}(0) + t\mathbf{z}(0) &+ \int_0^t\int_0^s \left[-\gamma \mathrm{e}^{-\gamma s_1}\mathbf{z}(s_1) + \gamma \mathbf{u}(s_1,\mathbf{x}(s_1))\right] \\ &\times \mathrm{d}s_1\mathrm{d}s + \sigma \int_0^t\int_0^s \mathrm{d}\mathbf{W}_{s_1}\mathrm{d}s, \end{aligned} \tag{8}$$

$$\begin{aligned} \mathbf{z}(t) = \mathbf{z}(0) + \gamma t\mathbf{u}(0,\mathbf{x}(0)) &+ \int_0^t\int_0^s \left[\gamma^2 \mathrm{e}^{\gamma s_1}\mathbf{u}(s_1,\mathbf{x}(s_1))\right. \\ &\left. + \gamma \mathrm{e}^{\gamma s_1}\frac{D\mathbf{u}(s_1,\mathbf{x}(s_1))}{Ds_1}\right]\mathrm{d}s_1\mathrm{d}s + \sigma \int_0^t \mathrm{e}^{\gamma s}\mathrm{d}\mathbf{W}_s, \end{aligned}$$

where

$$\frac{D}{Dt} = \frac{\partial}{\partial t} + (\mathbf{v}(t)\cdot\nabla) = \frac{\partial}{\partial t} + \mathrm{e}^{-\gamma t}(\mathbf{z}(t)\cdot\nabla)$$

is the material derivative. Applying the Itô formula (6) again, now to the integrands of (8), gives, after simplification:

$$\begin{aligned} \mathbf{x}(t) = \mathbf{x}(0) + t\mathbf{z}(0) &+ \frac{\gamma t^2}{2}[\mathbf{u}(0,\mathbf{x}(0)) - \mathbf{z}(0)] \\ &+ \gamma \int_0^t\int_0^s\int_0^{s_1}\left[\frac{D\mathbf{u}(s_2,\mathbf{x}(s_2))}{Ds_2} + \gamma \mathrm{e}^{-\gamma s_2}\mathbf{z}(s_2)\right. \\ &\left. - \gamma \mathbf{u}(s_2,\mathbf{x}(s_2))\right]\mathrm{d}s_2\mathrm{d}s_1\mathrm{d}s + \sigma \int_0^t\int_0^s \mathrm{d}\mathbf{W}_{s_1}\mathrm{d}s \\ &- \gamma\sigma \int_0^t\int_0^s\int_0^{s_1}\mathrm{d}\mathbf{W}_{s_2}\mathrm{d}s_1\mathrm{d}s_2, \end{aligned}$$

$$\mathbf{z}(t) = \mathbf{z}(0) + \gamma t\mathbf{u}(0,\mathbf{x}(0)) + \frac{t^2}{2}\Big[\gamma^2\mathbf{u}(0,\mathbf{x}(0)) + \gamma\frac{D\mathbf{u}(0,\mathbf{x}(0))}{Dt}\Big] + \int_0^t\int_0^s\int_0^{s_1}\Big[\gamma^3 e^{\gamma s_2}\mathbf{u}(s_2,\mathbf{x}(s_2)) + 2\gamma^2 e^{\gamma s_2}\frac{D\mathbf{u}(s_2,\mathbf{x}(s_2))}{Ds_2} + \gamma e^{\gamma s_2}\frac{D^2\mathbf{u}(s_2,\mathbf{x}(s_2))}{Ds_2^2}\Big] \times ds_2 ds_1 ds + \sigma\gamma\int_0^t\int_0^s\int_0^{s_1}(\nabla\mathbf{u}(s_2,\mathbf{x}(s_2)))\cdot d\mathbf{W}_{s_2} ds_1 ds + \sigma\int_0^t e^{\gamma s} d\mathbf{W}_s. \tag{9}$$

In the notation of [4], repeated application of the Itô chain rule to the **x** equation will give rise to multiple integrals of the form:

$$I_{(1,0)} = \int_0^t ds_0 \int_0^{s_0} dW_{s_1}, \tag{10}$$

$$I_{(1,0,0)} = \int_0^t ds_0 \int_0^{s_0} ds_1 \int_0^{s_1} dW_{s_2},$$

$$\cdots$$

$$I_{\underbrace{(1,0,\ldots,0)}_{n \text{ terms}}} = \int_0^t ds_0 \int_0^{s_0} ds_1 \cdots \int_0^{s_{n-2}} dW_{s_{n-1}}.$$

It can be shown ([4], Proposition 5.2.3) that

$$I_{(1,0)} = \int_0^t (t-s) dW_{s_0}, \tag{11}$$

$$I_{(1,0,0)} = \frac{1}{2}\int_0^t (t-s)^2 dW_{s_0},$$

$$\cdots$$

$$I_{\underbrace{(1,0,\ldots,0)}_{n \text{ terms}}} = \frac{1}{(n-1)!}\int_0^t (t-s)^{n-1} dW_{s_0}.$$

It follows that repeated application of the Itô chain rule to the **x** equation will converge to a single stochastic integral:

$$\frac{\sigma}{\gamma}\int_0^t [1 - e^{-\gamma(t-s)}] d\mathbf{W}_s. \tag{12}$$

The Itô–Taylor series expansion therefore gives the effective stochastic position and velocity terms:

$$\mathbf{R}_x = \frac{1}{\gamma}\int_0^t [1 - e^{-\gamma(t-s)}] d\mathbf{W}_s, \tag{13}$$

$$\mathbf{R}_v = \int_0^t e^{-\gamma(t-s)} d\mathbf{W}_s, \tag{14}$$

which are simply related [5]

$$\mathbf{R}_x(t) = \int_0^t \mathbf{R}_v(s)\, ds. \tag{15}$$

These terms have zero mean, and variances for time step h of:

$$\mathbb{E}(\mathbf{R}_x \otimes \mathbf{R}_x) = \mathbf{I}\int_0^h \frac{[1 - e^{-\gamma(h-s)}]^2}{\gamma^2} ds = \mathbf{I}\frac{2\gamma h - e^{-2\gamma h} + 4e^{-\gamma h} - 3}{2\gamma^3}, \tag{16}$$

$$\mathbb{E}(\mathbf{R}_v \otimes \mathbf{R}_v) = \mathbf{I}\frac{1 - e^{-2\gamma h}}{2\gamma}, \tag{17}$$

$$\mathbb{E}(\mathbf{R}_x \otimes \mathbf{R}_v) = \mathbf{I}\frac{(e^{-\gamma h} - 1)^2}{2\gamma^2}. \tag{18}$$

Numerically, these stochastic terms are constructed by assuming $\mathbf{R}_v = \sqrt{\mathbb{E}(R_v^2)}\mathbf{U}_1$, where $\mathbf{U}_1$ is a vector of Gaussian normal deviates. Then, $\mathbf{R}_x$ is given by $\mathbf{R}_x = b_1\mathbf{U}_1 + b_2\mathbf{U}_2$, where $\mathbf{U}_2$ is an independent vector of normal deviates, and constants b_1 and b_2 are:

$$b_1 = \frac{1}{\gamma}\tanh\left(\frac{\gamma h}{2}\right)\sqrt{\frac{1 - e^{-2\gamma h}}{2\gamma}}, \qquad b_2 = \frac{1}{\gamma}\sqrt{h - \frac{2}{\gamma}\tanh\left(\frac{\gamma h}{2}\right)} \tag{19}$$

in order that $\mathbf{R}_v$ and $\mathbf{R}_x$ obey (16)–(18).

Taking into account all of the above, and truncating high-order terms, we can write our integral equations of motion as:

$$\mathbf{x}(t+h) = \mathbf{x}(t) + [\mathbf{v}(t) - \mathbf{u}(t,x(t))]\frac{1 - e^{-\gamma h}}{\gamma} + \mathbf{u}(t,\mathbf{x}(t))h + \sigma\mathbf{R}_x, \tag{20}$$

$$\mathbf{v}(t+h) = \mathbf{v}(t)e^{-\gamma h} + \mathbf{u}(t,\mathbf{x}(t))(1 - e^{-\gamma h}) + \dot{\mathbf{u}}(t,\mathbf{x}(t))\frac{e^{-\gamma h} - 1 + \gamma h}{\gamma} + \sigma\mathbf{R}_v, \tag{21}$$

where $\dot{\mathbf{u}}$ is shorthand for $D\mathbf{u}/Dt$. Equation (20) is a special case of the result of Ermak and McCammon [3].

These discrete integral equations correspond exactly to the analytical solution of (4) under the assumptions of

(i) constant uniform $\mathbf{u}$, (ii) the absence of holonomic constraints and (iii) the fidelity of moments $\mathbf{R}_x$ and $\mathbf{R}_v$ to the assumed stochastic path. The recovery of this exact limit through the Duhamel form is the principal advantage of our method, and we will show that it provides stability in the limit $h\gamma > 1$ and helps control error in that limit.

By the theorem of [8], the omission of stochastic terms $\mathcal{O}(h^{5/2})$ and deterministic terms $\mathcal{O}(h^3)$ in our velocity equation gives a theoretical order of accuracy of 2 strong and 2 weak for systems (20) and (21).

Adding constraint forces into our integrator (20) and (21) leads to the following:

$$\mathbf{x}(t+h) = \mathbf{x}(t) + [\mathbf{v}(t) - \mathbf{u}(t, x(t))]\frac{1-\mathrm{e}^{-\gamma h}}{\gamma} + \mathbf{u}(t, \mathbf{x}(t))h + \sigma\mathbf{R}_x + \frac{1}{m}\mathbf{G}, \tag{22}$$

$$\mathbf{v}(t+h) = \mathbf{v}(t)\mathrm{e}^{-\gamma h} + \mathbf{u}(t, \mathbf{x}(t))(1-\mathrm{e}^{-\gamma h}) + \dot{\mathbf{u}}(t, \mathbf{x}(t))\frac{\mathrm{e}^{-\gamma h} - 1 + \gamma h}{\gamma} + \sigma\mathbf{R}_v + \frac{1}{m}\frac{1}{h}[\mathbf{G}^* + \mathbf{G}], \tag{23}$$

where $\mathbf{G}$ is given by (2) to ensure that condition (3) is obeyed at time $t+h$. $\mathbf{G}^*$ is computed in an analogous way to enforce condition:

$$\dot{\theta}_{\alpha\beta}(\mathbf{x}(t+h)) = (\dot{\mathbf{x}}_\alpha - \dot{\mathbf{x}}_\beta)\cdot(\mathbf{x}_\alpha - \mathbf{x}_\beta) = 0, \tag{24}$$

at time $t+h$. The force director $\nabla_{\mathbf{x}}\theta$ for $\mathbf{G}$ is $\Delta\mathbf{x}(t)$ and the force director $\nabla_{\mathbf{x}}\dot{\theta}$ for $\mathbf{G}^*$ is $\Delta\mathbf{x}(t+h)$. The Lagrange multipliers are determined by the RATTLE algorithm [1] or by the method of [2].

3. Results and conclusions

We demonstrate the convergence of our method in the strong and weak senses by the following procedures. The weak rate of convergence p_w of a process $\mathbf{y}$ is defined relative to an exact solution $\tilde{\mathbf{y}}$ by

$$|\mathbb{E}(\mathbf{y}(t)) - \mathbb{E}(\tilde{\mathbf{y}}(t))| \le Ch^{p_w}. \tag{25}$$

For our problem we do not have access to the exact solution, so we instead estimate p_w by Richardson extrapolation using the differences of solutions computed with different time steps h:

$$\boldsymbol{r}_\alpha^{(2h/h)} \equiv \left|\mathbb{E}(\mathbf{y}^{2h}(t)) - \mathbb{E}(\mathbf{y}^{h}(t))\right|, \tag{26}$$

and the rate of convergence is given by:

$$p = \log_2\left(\frac{\mathrm{r}_\alpha^{(4h/2h)}}{\mathrm{r}_\alpha^{(2h/h)}}\right). \tag{27}$$

For the weak measure of error, the particular paths (as defined by the moments $\mathbf{R}_x$ and $\mathbf{R}_v$) with resolutions h and $2h$ can be constructed independently.

Error in the strong sense is defined as

$$\mathbb{E}\|\mathbf{y}(t) - \tilde{\mathbf{y}}(t)\| \le Ch^{p_s}, \tag{28}$$

where $\|\cdot\|$ is some norm of the error over the paths sampled. We use the L_2 or RMS norm defined by

$$L_2(f) = \sqrt{\lim_{n\to\infty}\frac{1}{n}\sum_{i=1}^{n}|f_i|^2}. \tag{29}$$

As with the weak measure of error, we use Richardson extrapolation to deduce the rate p_s. However, in contrast to the weak measure, the computation with step $2h$ must be consistent with that at step h, as it is assumed that they are moments of the same underlying process. To enforce this consistency, we compute initially a sequence of moments $(\mathbf{R}_x)_h^n$ and $(\mathbf{R}_v)_h^n$ at the finest scale time scale h. The sequence of moments $(\mathbf{R}_v)_{2h}^n$, etc., are reconstructed from the sequence $(\mathbf{R}_v)_h^n$ by a coarsening procedure guided by the integral definition:

$$\begin{aligned}(\mathbf{R}_v)_{2h}^n &= \mathrm{e}^{-2h\gamma(n+1)}\int_{n(2h)}^{(n+1)(2h)}\mathrm{e}^{\gamma s}\mathrm{d}\mathbf{W}_s \\ &= \mathrm{e}^{-\gamma h}\mathrm{e}^{-h\gamma(2n+1)}\int_{n(2h)}^{(2n+1)h}\mathrm{e}^{\gamma s}\mathrm{d}\mathbf{W}_s \\ &\quad + \mathrm{e}^{-2h\gamma(n+1)}\int_{(2n+1)h}^{(n+1)(2h)}\mathrm{e}^{\gamma s}\mathrm{d}\mathbf{W}_s \\ &= \mathrm{e}^{-\gamma h}(\mathbf{R}_v)_h^{2n} + (\mathbf{R}_v)_h^{2n+1}.\end{aligned} \tag{30}$$

For $\mathbf{R}_x$ the same procedure yields

$$(\mathbf{R}_x)_{2h}^n = (\mathbf{R}_x)_h^{2n} + (\mathbf{R}_x)_h^{2n+1} + \frac{1-\mathrm{e}^{-\gamma h}}{\gamma}(\mathbf{R}_v)_h^{2n}. \tag{31}$$

These coarsening formulae are used recursively to construct moments for resolutions $4h$, etc., consistent with all higher resolution sequences.

Our first calculation demonstrates the advantage of the Duhamel form when γh is not negligible. We assume a weakly varying flow field $u_i = 10^{-3}\cos(10^{-3}x_i)$ (MKS), and choose $a = \|\Delta x\|_2 = 7\times10^{-6}\,\mathrm{m}$, $\gamma = 10^{10}\,\mathrm{s}^{-1}$ and $\sigma = 5\times10^3\,\mathrm{m/s}^{3/2}$ – parameters roughly corresponding to λ-phage DNA in a Kramers bead–rod abstraction. The initial conditions are $\mathbf{x}_0^0 = \mathbf{0}$, $\mathbf{x}_i^0 = \mathbf{x}_{i-1}^0 + a\mathbf{1}/\sqrt{3}$ and $\mathbf{v}_i^0 = \mathbf{u}(\mathbf{x}_i^0)$. The simulation is run to $10^{-9}\,\mathrm{s}$, so $\gamma h = 10^{-1}$ at the coarsest level of simulation. The calculation in 3D uses six particles connected in a linear topology. Expectations are assembled from 10^4 independent paths. Our stochastic terms are computed using uniformly distributed pseudorandom numbers generated by the

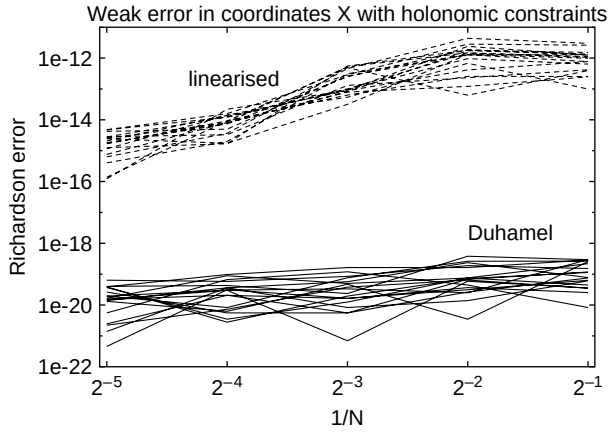

Figure 1. Comparison of linearised and Duhamel form results: weak coordinate error.

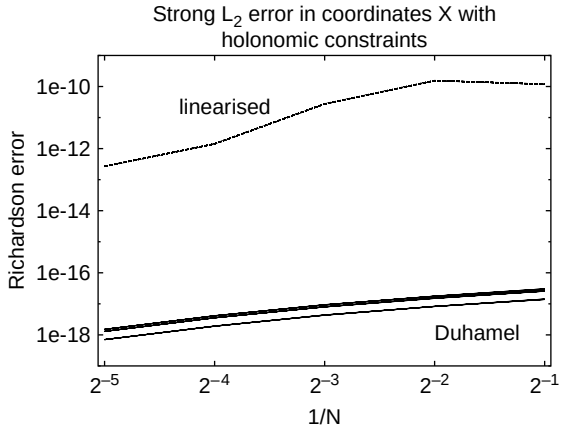

Figure 3. Comparison of linearised and Duhamel form results: strong coordinate error.

Mersenne Twister algorithm [6], converted to Gaussian normal deviates by the Box–Muller algorithm.

We compute weak and strong measures of error for our method, and for the linearised algorithm of Vanden-Eijnden and Ciccotti [13], using the same parameters and initial conditions. The results for all 18 coordinates and 18 velocities are presented in Figures 1–4.

Note that the Duhamel formulation leads to errors that are approximately six orders of magnitude smaller than that for the linearised method.

One reason our method displays significantly lower error as $\gamma h \approx 1$ can be appreciated by comparing the (co)variances in the Duhamel form (16)–(18) with the equivalent results in the linearised regime:

$$\mathbb{E}\left(\int_0^h \mathrm{d}s \int_0^s \mathrm{d}W\right)^2 = \frac{1}{3}h^3, \tag{32}$$

$$\mathbb{E}\left(\int_0^h \mathrm{d}W\right)^2 = h, \tag{33}$$

$$\mathbb{E}\left(\int_0^h \mathrm{d}W\right)\left(\left(\int_0^h \mathrm{d}s \int_0^s \mathrm{d}W\right)\right) = \frac{1}{2}h^2. \tag{34}$$

In the linearised versions, all of these stochastic terms grow without bound as h increases. In the Duhamel form, the variance of $\mathbf{R}_x$ grows linearly with h when $\gamma h \gg 1$ – the correct diffusion limit [3], versus as h^3 in the linearised result. However, the variance of $\mathbf{R}_v$ (17) and the covariance $\mathbb{E}(\mathbf{R}_v\mathbf{R}_x)$ (18) saturate, with asymptotic values of $1/(2\gamma)$ and $1/(2\gamma^2)$, respectively.

The effect of the unattenuated growth of these stochastic terms in the linearised equations is to compute velocity values subject to unphysically large variation. As a practical matter, this causes large violations of the constraints in each time step, and the linearised algorithm

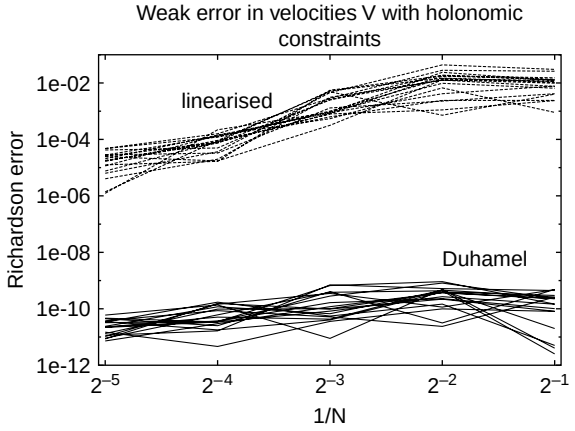

Figure 2. Comparison of linearised and Duhamel form results: weak velocity error.

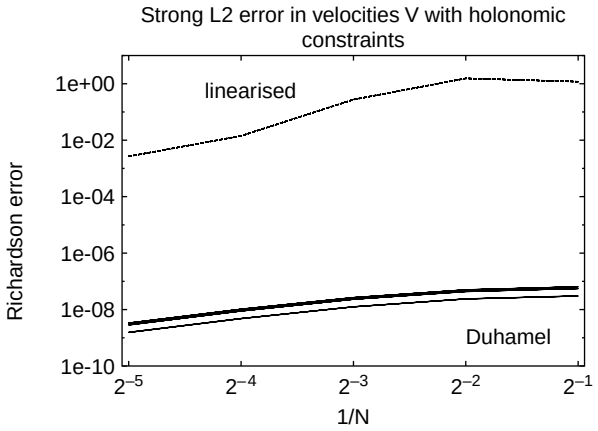

Figure 4. Comparison of linearised and Duhamel form results: strong velocity error.

fails for $\gamma h \approx 1$ (with the parameters described above) as a consequence of a failure of the nonlinear Lagrange force calculation to converge.

Another way to appreciate the time-step restriction on the linearised method is to consider velocity fluctuations for the simple ODE

$$\dot{\mathbf{v}} = -\gamma \mathbf{v} + \sigma \boldsymbol{\xi}, \tag{35}$$

which corresponds to our velocity equation for a single particle in a quiescent fluid, $\mathbf{u} = 0$. The mean squared velocity $\overline{\|\mathbf{v}\|}_2$ is given by the equipartition theorem to be $\sqrt{3k_BT/2m}$ or $(\sigma/2)\sqrt{3/\gamma}$. A discretisation of (35) by the linearised method of Vanden-Eijnden and Ciccotti carries a local discretisation error of $|\mathbf{v}|\gamma^3 h^2/6$ from the deterministic terms alone, and has a Lipschitz constant approximated by $\gamma|1 - \gamma h/2|$. The global discretisation error may be approximated at time T by [10]

$$\mathbf{e}(T) \leq \frac{|\mathbf{v}|\gamma^3 h^2}{6} \frac{\mathrm{e}^{\gamma|1-\gamma h/2|T} - 1}{\gamma|1 - \gamma h/2|}. \tag{36}$$

A condition for the suitability of the linearised approach is the requirement that $\mathbf{e} \ll \overline{\|\mathbf{v}\|}_2 \mathbf{1}$: the velocity solution error should be less than the average thermal velocity. Approximating $|\mathbf{v}|$ by $\overline{\|\mathbf{v}\|}_2 \mathbf{1}$, this inequality simplifies somewhat to

$$\frac{(\gamma h)^2}{6} \frac{\mathrm{e}^{|1-(\gamma h)/2|(\gamma T)} - 1}{|1 - (\gamma h)/2|} \ll 1,$$

which requires $\gamma h \ll 1$ for any T. For our model problem of λ-phage DNA, $\gamma \approx 10^{10}$/s, which means that the linearised technique yields acceptable results only for time steps significantly smaller than 10^{-10} s. This restriction is of no concern for atomic-scale MD simulations, where characteristic time steps are typically of order 10^{-15} s, but begins to be an issue for some discrete particle dynamics (DPD) simulations, where time steps approach 10^{-11} s [11]. We are primarily concerned with coarser scale simulations, where fluid dynamics are governed by characteristic time steps of 10^{-3}s, and the discretisation errors associated with a linearised approach are wholly unacceptable.

Because in the Duhamel form some of our stochastic terms saturate as $\gamma h \approx 1$, the asymptotic convergence limit is only seen for $\gamma h < 1$. With the physically based parameters used above, it is difficult to observe the theoretical asymptotic behaviour: the algorithm errors for these parameters and $\gamma h < 1$ are comparable with the numerical errors. Accordingly, to display the algorithm errors, we use the completely artificial parameters $a = 1$, $\gamma = 1$ and $\sigma = 10^{-1}$ with the fluid velocity field $\mathbf{u}$ and initial conditions as described in the previous example. We compute to time $T = 2$ ($\gamma T = 2$), again with 10^4 paths.

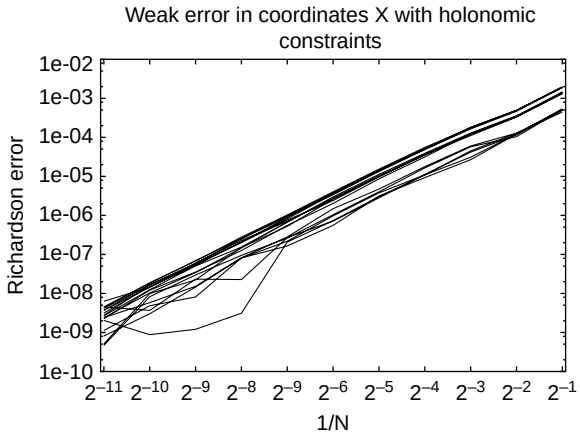

Figure 5. Convergence in weak coordinate error.

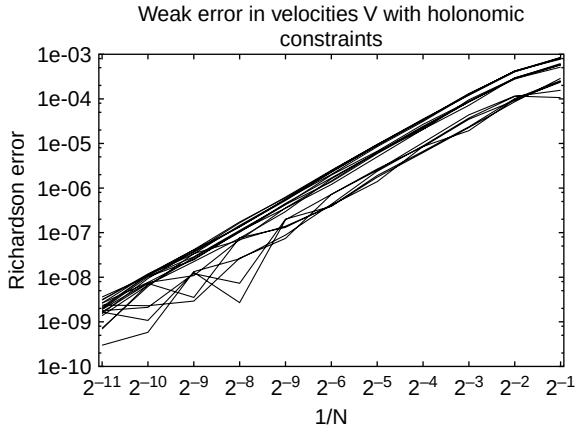

Figure 6. Convergence in weak velocity error.

The average weak and strong errors over the 18 respective variables are presented in Figures 5–8 and in Tables 1–4 with the rates of convergence. We observe 2-order accuracy in the weak sense and 1.5-order accuracy in the strong sense, for all variables.

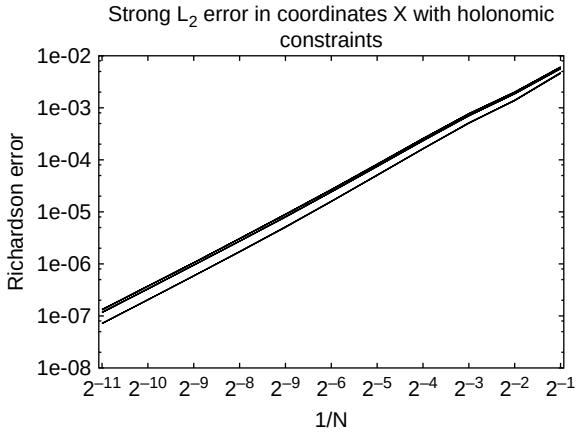

Figure 7. Convergence in strong coordinate error.

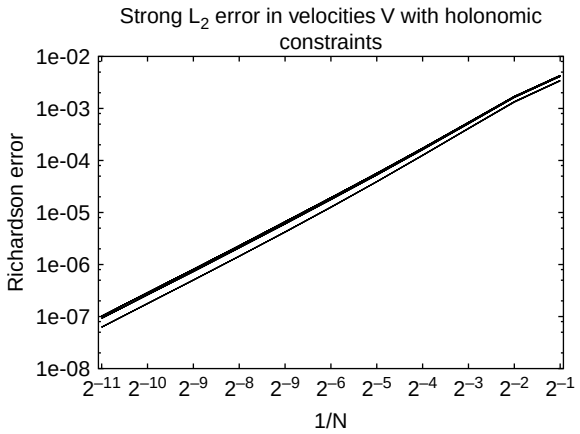

Figure 8. Convergence in strong velocity error.

Table 1. Average weak coordinate error and rate.

$N \propto 1/h$	Error $h/2\,h$	Rate
2048	2.89×10^{-9}	
1024	1.12×10^{-8}	1.96
512	3.96×10^{-8}	1.82
256	1.57×10^{-7}	1.99
128	6.07×10^{-7}	1.95
64	2.40×10^{-6}	1.98
32	9.30×10^{-6}	1.95
16	3.33×10^{-5}	1.84
8	1.13×10^{-4}	1.77
4	3.16×10^{-4}	1.48
2	1.28×10^{-3}	2.02

Table 2. Average weak velocity error and rate.

$N \propto 1/h$	Error $h/2h$	Rate
2048	1.95×10^{-9}	
1024	7.53×10^{-9}	1.95
512	2.48×10^{-8}	1.72
256	9.29×10^{-8}	1.91
128	3.65×10^{-7}	1.97
64	1.46×10^{-6}	2.00
32	5.77×10^{-6}	1.98
16	2.16×10^{-5}	1.90
8	8.06×10^{-5}	1.90
4	2.68×10^{-4}	1.73
2	5.38×10^{-4}	1.00

The second-order weak convergence, with holonomic constraints, can be explained by the analysis of [13]. However, it is noteworthy that the definition of second-order weak convergence differs amongst authors (cf. [4,9]), and a numerical test of the sort we present here does not verify that a given method is compatible with either definition. This is because $|\mathbb{E}(y) - \mathbb{E}(\tilde{y})|$ and $|\mathbb{E}(y + W) - \mathbb{E}(\tilde{y})|$ are indistinguishable, although y and $y + W$ differ fundamentally in the lowest order of stochastic contribution. This dilemma does not occur for the strong sense of error.

Table 3. Average strong L_2 coordinate error and rate.

$N \propto 1/h$	Error $h/2\,h$	Rate
2048	1.07×10^{-7}	
1024	3.03×10^{-7}	1.50
512	8.63×10^{-7}	1.51
256	2.50×10^{-6}	1.54
128	7.36×10^{-6}	1.56
64	2.23×10^{-5}	1.60
32	6.92×10^{-5}	1.64
16	2.17×10^{-4}	1.65
8	6.61×10^{-4}	1.60
4	1.75×10^{-3}	1.41
2	5.47×10^{-3}	1.64

Table 4. Average strong L_2 velocity error and rate.

$N \propto 1/h$	Error $h/2\,h$	Rate
2048	8.58×10^{-8}	
1024	2.43×10^{-7}	1.50
512	6.83×10^{-7}	1.49
256	1.95×10^{-6}	1.51
128	5.64×10^{-6}	1.53
64	1.66×10^{-5}	1.55
32	4.95×10^{-5}	1.58
16	1.53×10^{-4}	1.63
8	4.87×10^{-4}	1.67
4	1.56×10^{-3}	1.67
2	3.96×10^{-3}	1.35

The lower order observed in the strong sense can be understood as follows. If one expressed the constraint force as a continuous function of all $\mathbf{x}(t), \mathbf{v}(t)$, and expanded that constraint force in the Itô–Taylor fashion to second-order accuracy, terms proportional to

$$\mathrm{e}^{-\gamma h}\int_0^h \mathrm{e}^{-\gamma s_0}\mathrm{d}s_0 \int_0^{s_0} \mathrm{e}^{2\gamma s_1}\mathrm{d}s_1, \tag{37}$$

$$\mathrm{e}^{-\gamma h}\int_0^h \mathrm{d}s_0 \int_0^{s_0} \mathrm{e}^{\gamma s_1}\mathrm{d}W_{s_1}, \tag{38}$$

$$\mathrm{e}^{-\gamma t}\int_0^t \mathrm{e}^{-\gamma s_0}\mathrm{d}s_0 \int_0^{s_0} \mathrm{e}^{\gamma s_1}\mathrm{d}W^{\alpha}_{s_1} \int_0^{s_1} \mathrm{e}^{\gamma s_2}\mathrm{d}W^{\beta}_{s_2}, \tag{39}$$

$$\mathrm{e}^{-\gamma t}\int_0^t \mathrm{e}^{\gamma s_0}\mathrm{d}W^{\alpha}_{s_0} \int_0^{s_0} \mathrm{e}^{-\gamma s_1}\mathrm{d}s_1 \int_0^{s_1} \mathrm{e}^{\gamma s_2}\mathrm{d}W^{\beta}_{s_2}, \tag{40}$$

are discovered that are absent in the derivation of this paper. The first of these new integrals is deterministic and arises from a factor like $\partial^2 U/\partial X^2$ in (6). It is accounted for by an enforcement of constraints after a time step in the analysis of [13]. The second term equals $\mathbf{R}_x$ to $\mathcal{O}(h^{3/2})$, so to that order might be accounted for through the constraints. However, (39) and (40) are entirely new and cannot be expressed in terms of $\mathbf{R}_x, \mathbf{R}_v$, and therefore their omission in the explicit part of Equations (22) and (23) cannot be compensated through the Lagrange forces in (22) and (23). By the theorem of [8], terms of $\mathcal{O}(h^2)$ must

be included in a strong second-order method, hence the algorithm (22) and (23) is at most $\mathcal{O}(h^{3/2})$.

Work to develop a strong second-order method for the Langevin equations with holonomic constraints is in progress.

Acknowledgements

B. Kallemov was supported by the Bolashak scholarship of the President of the Republic of Kazakhstan. G.H. Miller was supported by LLNL IUT subcontracts number B550201 and number B553964, by DOE MICS contract number DE-FG02-03ER25579, and by NSF grant number DMS-0810939. Work at LLNL (D. Trebotich) was performed under the auspices of the U.S. Department of Energy by the University of California, Lawrence Livermore National Laboratory under contract No. W-7405-Eng-48.

Notes

1. Email: bkkallemov@ucdavis.edu
2. Email: treb@hpcrd.lbl.gov

References

[1] H.C. Andersen, *RATTLE: A "velocity" version of the SHAKE algorithm for molecular dynamics calculations*, J. Comp. Phys. 52 (1983), pp. 24–34.

[2] G. Ciccotti, M. Ferrario, and J.-P. Ryckaert, *Molecular dynamics of rigid systems in Cartesian coordinates. A general formulation*, Molec. Phys. 47 (1982), pp. 1253–1264.

[3] D.L. Ermak and J.A. McCammon, *Brownian dynamics with hydrodynamic interactions*, J. Chem. Phys. 69 (1978), pp. 1352–1360.

[4] P.E. Kloeden and E. Platen, *Numerical Solution of Stochastic Differential Equations*, Springer, New York, 1999.

[5] D.F. Kuznetsov, *Stochastic Differential Equations: Theory and Practice of Numerical Solution*, 2nd ed., St. Petersburg, Polytechnical University Press, St. Petersburg, Russia, 2007.

[6] M. Matsumoto and T. Nishimura, *Mersenne Twister: A 623-dimensionally equidistributed uniform pseudorandom number generator*, ACM Trans. Model. Comp. Simul. 8 (1998), pp. 3–30.

[7] G.H. Miller and D. Trebotich, *Toward a mesoscale model for the dynamics of polymer solutions*, J. Comp. Theor. Nanosci. 4 (2007), pp. 1–5.

[8] G.N. Milstein, *A theorem on the order of convergence of mean-square approximations of solutions of system of stochastic differential equations*, Theory Prob. Appl. 32 (1988), pp. 738–741.

[9] G.N. Milstein and M.V. Tretyakov, *Stochastic Numerics for Mathematical Physics*, Springer, New York, 2004.

[10] J. Stoer and R. Bullirsch, *Introduction to Numerical Analysis*, 2nd ed., Springer, New York, 1993.

[11] V. Symeonidis and G.E. Karniadakis, *A family of time-staggered schemes for integrating hybrid DPD models for polymers: Algorithms and applications*, J. Comp. Phys. 218 (2006), pp. 82–101.

[12] D. Trebotich, G.H. Miller, P. Colella, D.T. Graves, D.F. Martin, and P.O. Schwartz, *A tightly coupled particle-fluid model for DNA-laden flows in complex microscale geometries*, Comput. Fluid Solid Mech. 2005 (2005), pp. 1018–1022.

[13] E. Vanden-Eijnden and G. Ciccotti, *Second-order integrators for Langevin equations with holonomic constraints*, Chem. Phys. Lett. 429 (2006), pp. 310–316.